AMERICAN SOCIETY FOR MICROBIOLOGY | Journal of Clinical Microbiology®

MYCOBACTERIOLOGY AND AEROBIC ACTINOMYCETES

Genetic Mimetics of *Mycobacterium tuberculosis* and Methicillin-Resistant *Staphylococcus aureus* as Verification Standards for Molecular Diagnostics

Edith Erika Machowski,[a] Bavesh Davandra Kana[a,b]

DST/NRF Centre of Excellence for Biomedical TB Research, School of Pathology, Faculty of Health Sciences, University of the Witwatersrand and the National Health Laboratory Service, Johannesburg, South Africa[a]; MRC-CAPRISA HIV-TB Pathogenesis and Treatment Research Unit, Centre for the AIDS Programme of Research in South Africa, Durban, South Africa[b]

ABSTRACT Molecular diagnostics have revolutionized the management of health care through enhanced detection of disease or infection and effective enrollment into treatment. In recognition of this, the World Health Organization approved the rollout of nucleic acid amplification technologies for identification of *Mycobacterium tuberculosis* using platforms such as GeneXpert MTB/RIF, the GenoType MTBDR*plus* line probe assay, and, more recently, GeneXpert MTB/RIF Ultra. These assays can simultaneously detect tuberculosis infection and assess rifampin resistance. However, their widespread use in health systems requires verification and quality assurance programs. To enable development of these, we report the construction of genetically modified strains of *Mycobacterium smegmatis* that mimic the profile of *Mycobacterium tuberculosis* on both the GeneXpert MTB/RIF and the MTBDR*plus* line probe diagnostic tests. Using site-specific gene editing, we also created derivatives that faithfully mimic the diagnostic result of rifampin-resistant *M. tuberculosis*, with mutations at positions 513, 516, 526, 531, and 533 in the rifampin resistance-determining region of the *rpoB* gene. Next, we extended this approach to other diseases and demonstrated that a *Staphylococcus aureus* gene sequence can be introduced into *M. smegmatis* to generate a positive response for the SCC*mec* probe in the GeneXpert SA Nasal Complete molecular diagnostic cartridge, designed for identification of methicillin-resistant *S. aureus*. These biomimetic strains are cost-effective, have low biohazard content, accurately mimic drug resistance, and can be produced with relative ease, thus illustrating their potential for widespread use as verification standards for diagnosis of a variety of diseases.

KEYWORDS GeneXpert, Hain MTBDRplus, *Mycobacterium smegmatis*, *Mycobacterium tuberculosis*, *Staphylococcus aureus*, biomimicry, molecular diagnostics, rifampin resistance, tuberculosis

Received 13 July 2017 **Returned for modification** 10 August 2017 **Accepted** 14 September 2017

Accepted manuscript posted online 20 September 2017

Citation Machowski EE, Kana BD. 2017. Genetic mimetics of *Mycobacterium tuberculosis* and methicillin-resistant *Staphylococcus aureus* as verification standards for molecular diagnostics. J Clin Microbiol 55:3384–3394. https://doi.org/10.1128/JCM.01111-17.

Editor Geoffrey A. Land, Carter BloodCare & Baylor University Medical Center

Address correspondence to Bavesh Davandra Kana, bavesh.kana@nhls.ac.za.

Tuberculosis (TB) is a devastating disease that has afflicted humankind for millennia and persists because of ongoing transmission, various socioeconomic reasons, poor infection control, drug resistance, and diagnostic challenges (1). Diagnosis of TB has traditionally been based on symptoms, together with methods such as smear microscopy and culture on solid or in liquid media (2). The current "gold standard" for TB diagnosis remains the isolation of *Mycobacterium tuberculosis* in culture, whether on solid media (Lowenstein-Jensen slants or Middlebrook 7H10 agar) or in liquid media (in the Bactec MGIT 960 system) (3). However, due to the low growth rate of *M. tuberculosis in vitro*, lengthy culture times are required to obtain a result. This diagnostic delay is compounded if phenotypic drug susceptibility testing is required to confirm resistance.

These challenges fuel transmission, lead to delays in linkage to care, and can result in treatment with ineffective antibiotics (4, 5).

The introduction of molecular diagnostics has challenged traditional paradigms for disease detection, resulting in the global use of these platforms for both communicable and noncommunicable diseases (6). However, these effects have yet to fully accrue with TB. Current nucleic acid amplification technologies (NAATs) can simultaneously detect *M. tuberculosis* and probe for antibiotic resistance on a variety of samples, including sputum (7). The World Health Organization has endorsed the introduction and scale-up of two such NAAT diagnostic assays for TB (6). The GeneXpert MTB/RIF system utilizes molecular beacon technology that monitors fluorescence based on real-time PCR amplification and provides a quantitative measure of bacillary load, in addition to profiling rifampin (RIF) resistance. Recently, a more sensitive version of this platform, the GeneXpert MTB/RIF Ultra, was launched for global use. The line probe assay (LPA) (Genotype MTBDR*plus* assay; HAIN Life Sciences, Germany) identifies specific *M. tuberculosis* alleles that are associated with RIF and isoniazid (INH) resistance using hybridization technology. Additionally, this platform is used for species identification of the *M. tuberculosis* complex (MTBC) and nontuberculous mycobacteria. A key feature to successful implementation of these technologies is the presence of robust quality assurance programs. An example of this is illustrated by the use of dried culture spots (DCSs), containing inactivated *M. tuberculosis*, to verify GeneXpert units (6, 8).

In light of this, the availability of verification material that accurately mimics sputum-derived *M. tuberculosis* will allow for the opportunity to develop fine-tuned verification programs at a national and possibly even global level. To facilitate this, we undertook to produce a new generation of verification reagents that can be easily scaled in the health systems of countries where TB is endemic. In addition, the rapid emergence of drug-resistant TB creates the need for verification standards that reflect prevalent rifampin resistance genotypes found in the clinical setting. In this study, we attempt to address some of these issues through the generation of genetically altered strains of the nonpathogenic bacterium *Mycobacterium smegmatis*—a relative of *M. tuberculosis*—that can serve as biomimetics of drug-sensitive and drug-resistant *M. tuberculosis*. These biomimetic strains faithfully mimicked *M. tuberculosis* when applied to GeneXpert-MTB or the MTBDR*plus* assays and circumvent any safety concerns that may have arisen through the use of pathogenic *M. tuberculosis* in previous verification programs. To demonstrate the broad applicability of our approach, another *M. smegmatis* biomimetic derivative was produced by introduction of a nucleotide sequence from methicillin-resistant *Staphylococcus aureus* (MRSA). This strain produced the expected result when applied to the GeneXpert SA Nasal Complete molecular diagnostic cartridge (GeneXpert-SANC) and can now be used as a quality assurance verification reagent for the diagnosis of MRSA infection. The advantages of the biomimetics generated in this study include low cost of production, relatively low biohazard content, and accurate mimicking of drug resistance, all of which poise them for widespread use in the clinical context.

RESULTS

Construction of *M. tuberculosis* biomimetics. The genetic determinants for RIF resistance in most clinical isolates of *M. tuberculosis* map to an 81-bp region of the *rpoB* gene, termed the RIF resistance-determining region ($RRDR_{TB}$). To enhance detection of TB disease and rifampin resistance, the $RRDR_{TB}$ (Fig. 1A) serves as the molecular target for the GeneXpert and MTBDR*plus* NAAT systems. We sought to use *M. smegmatis* to construct *M. tuberculosis* biomimetics, an approach that was based on the premise that *M. smegmatis* would not be erroneously detected by the GeneXpert or LPA assays as *M. tuberculosis*. Hence, we first set out to compare the *M. smegmatis* mc^2155 RRDR ($RRDR_{SM}$) and $RRDR_{TB}$. The $RRDR_{SM}$ differs from its *M. tuberculosis* counterpart at 9 positions (Fig. 1A). The presence of these single nucleotide polymorphisms (SNPs) results in the inability of probes A, B, D, and E to bind to the $RRDR_{SM}$ during PCR. A positive result is obtained from probe C due to 16 bp of 100% homology at this location

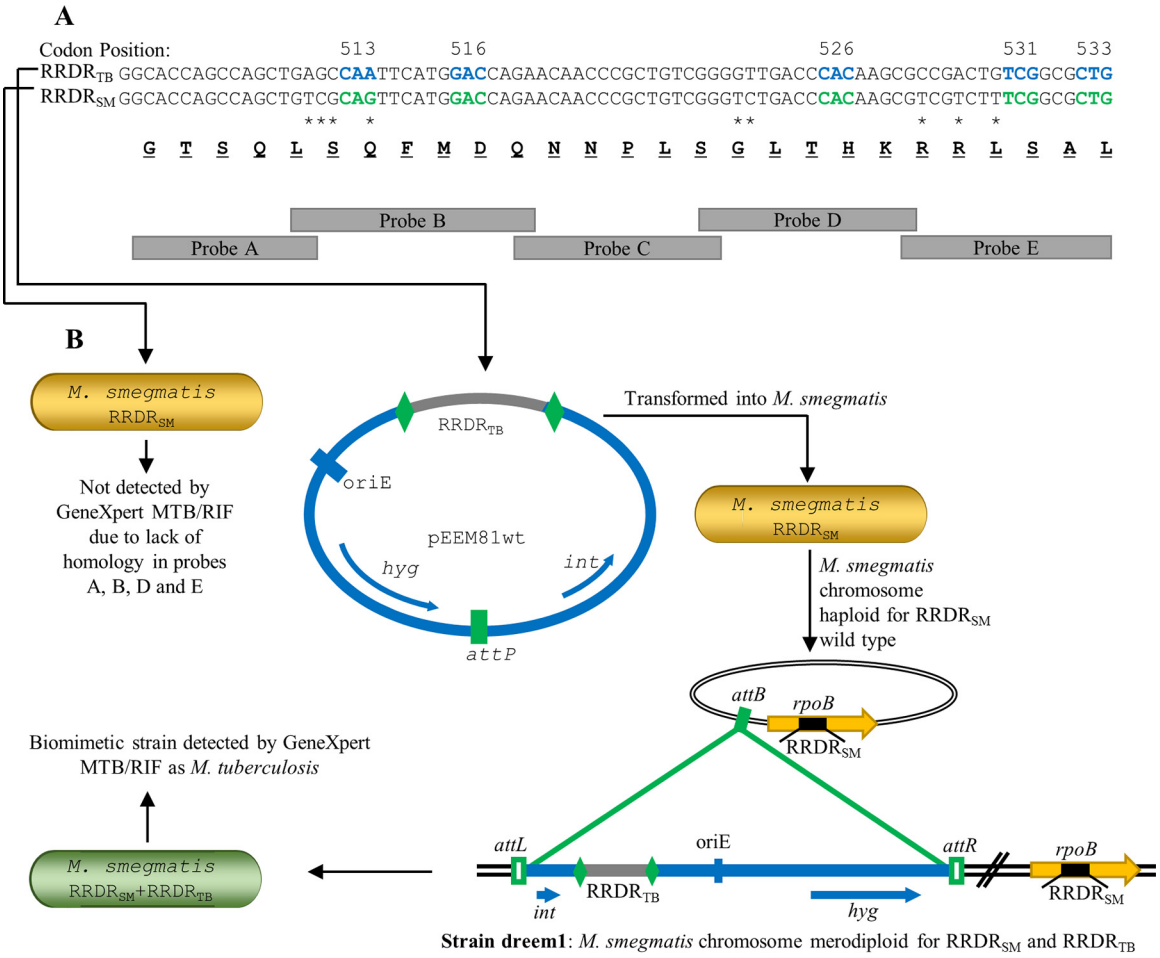

FIG 1 Construction of an *M. tuberculosis*-biomimetic strain. (A) Alignment of the 81-bp RRDRs from *M. tuberculosis* (RRDR$_{TB}$) and *M. smegmatis* (RRDR$_{SM}$). Asterisks indicate SNP differences between RRDR$_{TB}$ and RRDR$_{SM}$. All SNPs in this region are synonymous; as a result, the peptide sequence is the same in both cases. Light blue text, RRDR$_{TB}$ codons of clinical relevance; green text, RRDR$_{SM}$ corresponding codons; underlined text, amino acid residues. Shown also are the probes from the GeneXpert MTB/RIF. Mycobacterial nucleotide sequences were obtained from the MycoBrowser website (http://mycobrowser.epfl.ch/). Probe C has 100% homology with both RRDRs. (B) Construction of *M. tuberculosis* biomimetic. The RRDR$_{TB}$ was cloned into a shuttle plasmid to yield pEEM81wt, which was inserted into *M. smegmatis* mc^{2}155. Green diamonds, pUC57-Simple multiple-cloning sites. Integration at the *attB* site resulted in strain dreem1, which is a partial merodiploid, carrying both RRDRs. The presence of the RRDR$_{TB}$ in *M. smegmatis* leads to GeneXpert MTB/RIF reading this biomimetic strain as drug-sensitive *M. tuberculosis*.

of the RRDR (Fig. 1A; Table 1). As a consequence, mc^{2}155 is classified as "MTB not detected" (MTBN) by GeneXpert (Fig. 1B; Table 1) and provides an ideal genetic background for building *M. tuberculosis* biomimetics. To test this, the RRDR$_{TB}$ was cloned into a shuttle plasmid which was introduced into *M. smegmatis* mc^{2}155 using the L5-mycobacteriophage integrating system, a well-established method for gene delivery in mycobacteria (Fig. 1B) (9). In this case, the attachment site *attP* carried on the plasmid recombines with the complementary *attB* in the bacterial chromosome, facilitated by the integrase gene (*int*), also carried on the plasmid. As a result, hybrid *attL* and *attR* sites remain as scars flanking the delivered sequence (Fig. 1B). This approach resulted in *M. smegmatis* strain dreem1, which carried a perfect match to the RRDR$_{TB}$ and was classified as "*M. tuberculosis* detected" (MTBD) by GeneXpert MTB/RIF (Table 1). Introduction of RRDR$_{TB}$ in strain dreem1 against the background of the RRDR$_{SM}$ resulted in partial merodiploidy that was not identified by GeneXpert MTB/RIF, thus increasing the specificity of our approach (Table 1). We further tested dilutions of dreem1 cultures and confirmed that a specific positive result was obtained from GeneXpert MTB/RIF in all cases and that the result was quantitatively consistent, i.e., higher cell densities yielded lower cycle thresholds (C_T) as expected (Table 1).

TABLE 1 Test results from GeneXpert MTB/RIF

Strain	$RRDR_{TB}$ mutation	Dilution factor	MTB result[a]	RIF^r	C_T with[b]: Probe A	Probe B (513 Q→L, 516 D→V)	Probe C	Probe D (526 H→Y)	Probe E (531 S→L, 533 L→P)
mc^2155		10^4	MTBN	NA	*	*	29	*	*
dreem1	None (wild type)	10^3	MTBD-M	No	18	20	18	20	20
		10^4	MTBD-L	No	22	25	23	24	23
		10^5	MTBD-L	No	25	25	24	25	25
dreem2	513 Q→L(CAA→CTA)	10^2	MTBD-H	Yes	15	*	15	16	17
		10^3	MTBD-M	Yes	21	*	22	23	23
		10^4	MTBD-L	No	24	27[c]	25	26	26
dreem3	516 D→V(GAC→GTC)	10^2	MTBD-H	Yes	11	*	11	13	13
		10^3	MTBD-H	Yes	16	*	17	18	18
		10^4	MTBD-M	Yes	21	41	21	22	22
dreem4	526 H→Y(CAC→TAC)	10^2	MTBD-H	Yes	13	15	13	*	15
		10^3	MTBD-M	Yes	17	20	17	*	17
		10^4	MTBD-M	Yes	21	24	22	*	22
dreem5	531 S→L(TCG→TTG)	10^2	MTBD-H	Yes	15	17	16	17	*
		10^3	MTBD-M	Yes	19	21	20	21	*
		10^4	MTBD-M	Yes	22	23	22	23	*
dreem6	533 L→P(CTG→CCG)	10^2	MTBD-H	Yes	14	16	15	16	*
		10^3	MTBD-M	Yes	18	19	18	19	25
		10^4	MTBD-M	Yes	20	22	21	22	26

[a]GeneXpert diagnostic output. MTBN, *M. tuberculosis* not detected; MTBD-L, *M. tuberculosis* detected, low; MTBD-M, *M. tuberculosis* detected, medium; MTBD-H, *M. tuberculosis* detected, high.

[b]Shading indicates probe failure. *, C_T values above the computational cutoff values defined for that probe. Where bacterial numbers are low, large C_T values can be background signal.

[c]At low cell densities, C_T values that approach the cutoff limit can be compensated for by the GeneXpert computational program taking into account comparative signals obtained from all five probes.

Having successfully created an *M. tuberculosis*-biomimetic verification standard for the wild-type (WT) $RRDR_{TB}$ in GeneXpert MTB/RIF, we next turned our attention to drug resistance. Within the 81-bp sequence of the $RRDR_{TB}$, specific SNPs linked to RIF resistance in clinical isolates were identified (Fig. 2A) (10, 11). These nonsynonymous substitutions prevent RIF from binding the β-subunit of the RNA polymerase (RpoB) (12), thereby restoring the ability to synthesize RNA in the presence of the drug, resulting in phenotypic RIF resistance. Five SNPs were selected, positioned at probes B, D, and E, namely, 513 Q→L, 516 D→V, 526 H→Y, 531 S→L, and 533 L→P, for building biomimetics of RIF-resistant *M. tuberculosis* (Fig. 2A) (11, 13). These SNPs were individually engineered into the $RRDR_{TB}$ and the resulting plasmids (Table 2) were introduced into wild-type *M. smegmatis* mc^2155 to create strains dreem2 to dreem6 (Fig. 2A and Table 2). In each of these cases, the introduction of SNPs should result in loss of sequence complementarity to a particular probe in the GeneXpert MTB/RIF, leading to failure of the probe to bind, an event that is interpreted by the GeneXpert as the presence of RIF-resistant *M. tuberculosis*. As expected, all drug-resistant mimetic strains of *M. smegmatis* were scored as RIF-resistant *M. tuberculosis* by GeneXpert, and in all cases, the expected probe dropouts were observed (Table 1). With the exception of dreem2, the diagnostic pickup of RIF-resistant *M. tuberculosis* occurred across all dilutions tested, pointing to substantive robustness in the ability of these strains to serve as verification reagents for drug-resistant TB (Table 1). With strain dreem2, in the presence of very low numbers of organisms ($C_T = 24$), GeneXpert was able to detect *M. tuberculosis* but miscalled the presence of resistance. This is probably due to the small difference in C_T values between all the probes under these conditions.

Application of *M. tuberculosis*-biomimetic strains in the LPA. The Hain MTBDR*plus* LPA also uses the *rpoB* region to detect RIF resistance in *M. tuberculosis* while also

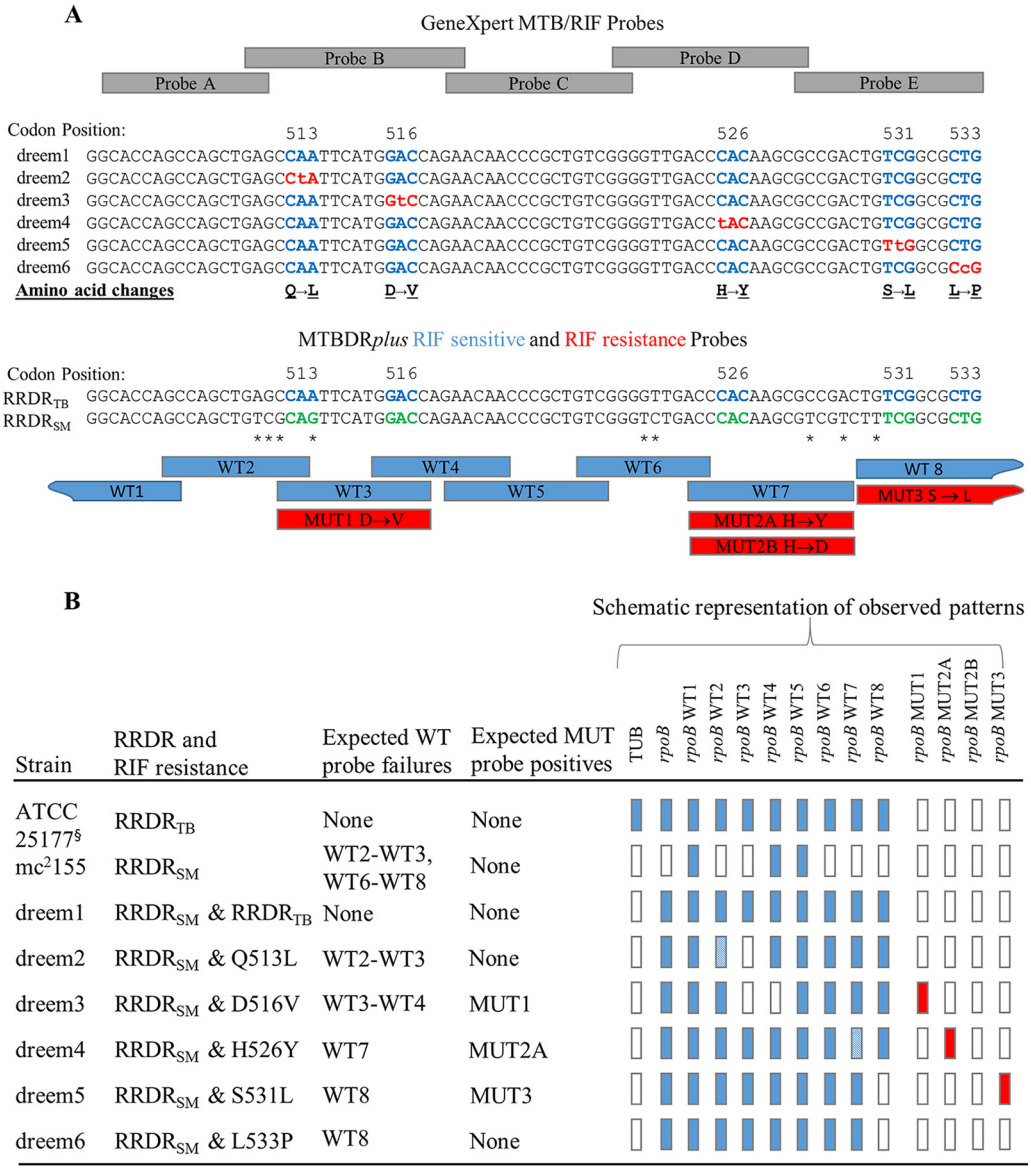

Strain	RRDR and RIF resistance	Expected WT probe failures	Expected MUT probe positives
ATCC 25177§	$RRDR_{TB}$	None	None
mc^2155	$RRDR_{SM}$	WT2-WT3, WT6-WT8	None
dreem1	$RRDR_{SM}$ & $RRDR_{TB}$	None	None
dreem2	$RRDR_{SM}$ & Q513L	WT2-WT3	None
dreem3	$RRDR_{SM}$ & D516V	WT3-WT4	MUT1
dreem4	$RRDR_{SM}$ & H526Y	WT7	MUT2A
dreem5	$RRDR_{SM}$ & S531L	WT8	MUT3
dreem6	$RRDR_{SM}$ & L533P	WT8	None

FIG 2 Construction of RIF-resistant *M. tuberculosis* biomimetics. (A) Alignment of the wild-type (dreem1) and RIF-resistant (dreem2 to dreem6) $RRDR_{TB}$ variants. Light blue text, wild-type $RRDR_{TB}$ codons of clinical relevance; red text, mutant codons. Underlined text indicates amino acid changes. Gray boxes above indicate binding regions for the GeneXpert MTB/RIF probes. Also shown at the bottom is the alignment of the $RRDR_{TB}$ and $RRDR_{SM}$ (green text, $RRDR_{SM}$ corresponding codons) and the binding regions of MTBDR*plus* LPA wild-type (WT) or mutant (MUT) probes. Probes WT1, WT4, and WT5 have 100% homology with the $RRDR_{TB}$ and $RRDR_{SM}$ and hence are able to bind *M. smegmatis* DNA. Probes WT1 and WT8 extend beyond the 81-bp RRDR. (B) Schematic representation of LPA hybridization results. A positive result in the TUB probe identifies a strain as belonging to the *M. tuberculosis* complex (MTBC). No TUB hybridization was seen in the *M. smegmatis*-based strains. Light blue boxes indicate positive hybridization for WT probes, white boxes indicate the absence of hybridization, and hatched boxes indicate intermediate hybridization. Red boxes indicate positive hybridization by MUT probes. Resistance profiling is shown only for RIF. Results are not shown for controls CC and AC or for INH targets of the LPA. §, ATCC 25177, a strain of *Mycobacterium bovis* BCG, contains the exact match for the RRDR in *M. tuberculosis*.

probing for INH resistance at the *inhA* and *katG* regions of the genome. The operational procedure to test for RIF resistance by the LPA involves hybridization of different probes to the *rpoB* region, the detection of which confirms *M. tuberculosis* infection and RIF resistance. A total of 8 probes target the wild-type *rpoB* region (labeled WT1 to WT8, covering 95 bp [Fig. 2A]); these allow for distinguishing between RIF-susceptible and RIF-resistant strains. An additional probe (labeled TUB in Fig. 2B) is used for species identification of organisms that belong to the *M. tuberculosis* complex (MTBC). As expected, the TUB probe failed to detect *M. smegmatis*, while probes WT1 (partially

TABLE 2 Strains and plasmids used in this study

Plasmid or strain	Description, markers, and/or genotype	Reference or source
Plasmids		
pHINT	*oriE*; *bla*; *hyg*; L5-attP-*int*	31
pEEM81wt	Composite shuttle plasmid combining the *oriE* and $RRDR_{TB}$ from a pUC57-based vector with *hyg*; L5-*attP-int* resistance and integrating elements from pHINT	This study
pEEM513	Composite shuttle plasmid analogous to pEEM81wt, bearing Q513L	This study
pEEM516	Composite shuttle plasmid analogous to pEEM81wt, bearing D516V	This study
pEEM526	Composite shuttle plasmid analogous to pEEM81wt, bearing H526Y	This study
pEEM531	Composite shuttle plasmid analogous to pEEM81wt, bearing S531L	This study
pEEM533	Composite shuttle plasmid analogous to pEEM81wt, bearing L533P	This study
pEEMSCC	Composite shuttle plasmid combining *oriE* and SCC*mec* from a pUC57-based vector with *hyg*; L5-*attP-int* resistance and integrating elements from pHINT	This study
Strains		
Escherichia coli DH5α	*fhuA2 lacΔU169 phoA glnV44 Φ80′ lacZΔM15 gyrA96 recA1 relA1 endA1 thi-1 hsdR17*	Promega
M. smegmatis mc^2155	*ept*-1; high-frequency transformation mutant of *M. smegmatis* ATCC 607	32
dreem1	Derivative of mc^2155 with pEEM81wt integrated at *attB*; Hyg^r, bearing the $RRDR_{SM}$ and the wild-type $RRDR_{TB}$ allele	This study
dreem2	Derivative of mc^2155 analogous to dreem1, bearing the $RRDR_{SM}$ and the Q513L $RRDR_{TB}$ allele	This study
dreem3	Derivative of mc^2155 analogous to dreem1, bearing the $RRDR_{SM}$ and the D516V $RRDR_{TB}$ allele	This study
dreem4	Derivative of mc^2155 analogous to dreem1, bearing the $RRDR_{SM}$ and the H526Y $RRDR_{TB}$ allele	This study
dreem5	Derivative of mc^2155 analogous to dreem1, bearing the $RRDR_{SM}$ and the S531L $RRDR_{TB}$ allele	This study
dreem6	Derivative of mc^2155 analogous to dreem1, bearing the $RRDR_{SM}$ and the L533P $RRDR_{TB}$ allele	This study
dreemX	Derivative of mc^2155, with pEEMSCC integrated at *attB*; Hyg^r, bearing SCC*mec*	This study

outside the RRDR), WT4, and WT5 bound to *M. smegmatis* DNA due to 100% sequence homology in these regions (Fig. 2). Probes WT2, WT3, WT6, WT7, and WT8 failed to bind to *M. smegmatis* genomic DNA due to lack of homology. Given these differences between the performance of the LPA on *M. tuberculosis* (H37Rv) and *M. smegmatis* mc^2155, we reasoned that our biomimetics may partially recapitulate *M. tuberculosis* and RIF resistance on the LPA. As expected, DNA from strain dreem1 was detected by probes WT1 to WT8, providing a result that is highly similar to that of *M. tuberculosis*, suggesting that with the exception of the TUB probe, dreem1 recapitulates *M. tuberculosis* on the LPA for the *rpoB* locus (Fig. 2B). For RIF resistance, strains dreem2 to dreem6 yielded the expected probe dropouts for all WT probes and the expected probe hybridizations for mutant (MUT) probes (Fig. 2B). In some cases, instead of complete probe dropout, a faint band was observed, but it was clearly discernible from positive hybridization. In strains dreem3, dreem4, and dreem5, the presence of the mutant alleles was positively identified by hybridizing bands with the respective SNPs as expected: MUT1 (D516V), MUT2A (H526Y), and MUT3 (S531L) (Fig. 2B). No bands were obtained for the INH loci, namely, *katG* and *inhA*, indicating divergence at these regions between *M. tuberculosis* and *M. smegmatis* (data not shown).

Construction of a biomimetic strain for *S. aureus*. We next attempted to extend our biomimicry approach to develop verification reagents for another bacterium, MRSA. Antibiotic resistance in *S. aureus* is acquired by horizontal gene transfer of the staphylococcal cassette chromosome *mec* (SCC*mec*), which is able to rapidly disseminate genes within populations and exists in a multitude of configurations with respect to the genetic payload (14). The archetypal SCC*mec* is a circular mobile element that contains the *mecA* gene, encoding the penicillin-binding protein 2b (PBP2b), responsible for methicillin resistance (15). Analogous to insertion of L5-mycobacteriophage-based vectors at *attB*, the circular SCC*mec* element integrates by attachment of a distinct $attP_{SCC}$ sequence to that of the bacterial $attB_{SCC}$, located at *orfX* (reannotated to *rlmH* [16]) in the chromosome (Fig. 3A). This is mediated by the associated serine recombinases encoded by *ccrAB* (17). The GeneXpert-SANC test targets three loci in the *S. aureus* chromosome. It probes for the gene encoding staphylococcal protein A (*spa*), which identifies *S. aureus* infection. It also probes for the *mecA* gene to determine whether it is present in the SCC*mec* integrating element, as there are SSC*mec* elements lacking the *mecA* gene. Additionally, the GeneXpert-SANC probes for the SCC*mec*

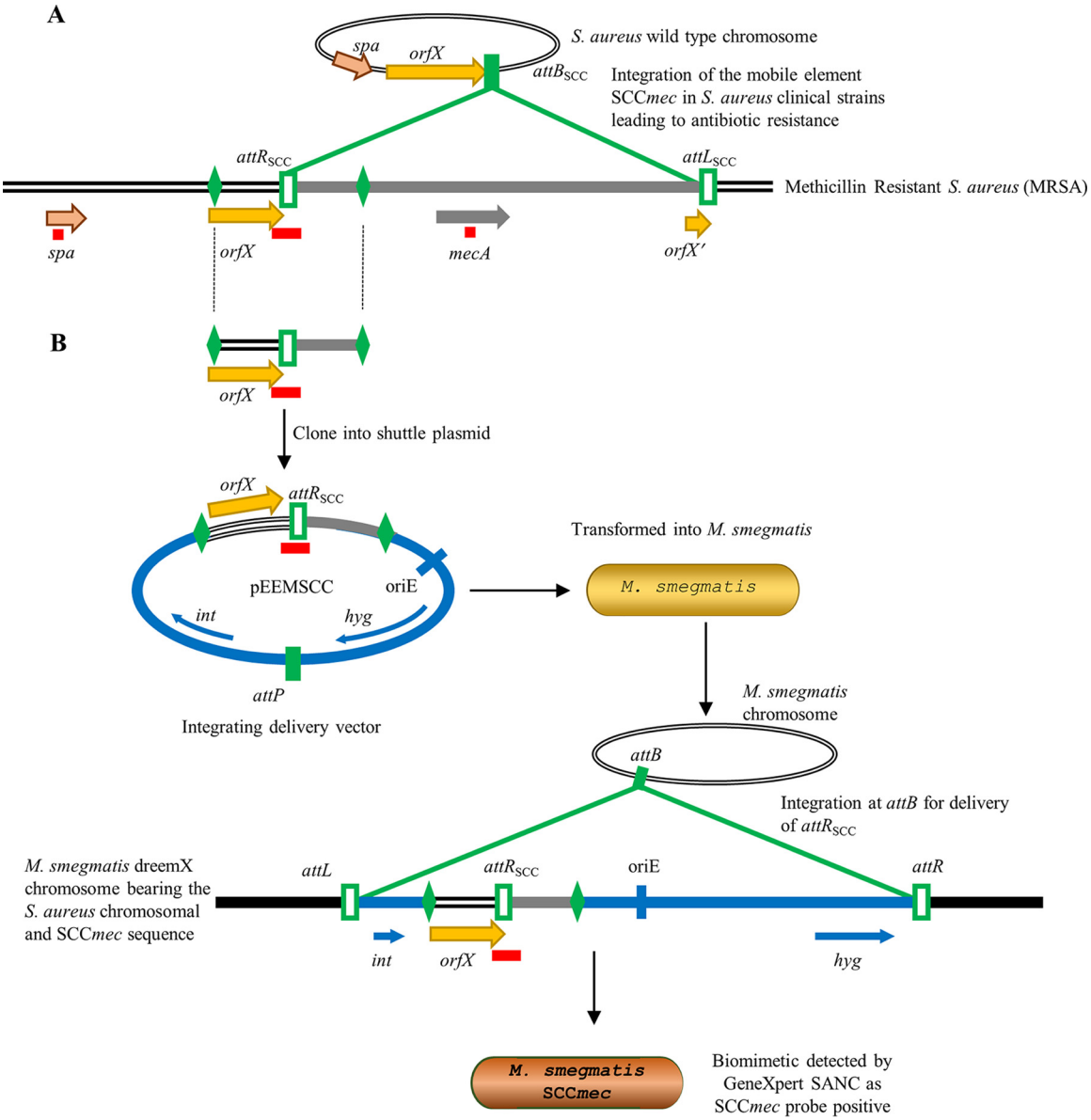

FIG 3 Construction of an *S. aureus*-biomimetic strain. (A) Chromosomal configuration of wild-type *S. aureus*. The $attB_{SCC}$ site at which SCC*mec* integrates is located at the 3′ end of *orfX*, overlapping the stop codon. The *spa* locus, which is used for species identification, is distal to *orfX*. Shown is the integration of an SCC*mec* element into wild-type *S. aureus*, resulting in the production of a MRSA strain. (B) A 960-bp fragment containing the entire *orfX* open reading frame (480 bp) and further 480 bp downstream of SCC*mec* sequence was configured into a shuttle plasmid to yield pEEMSCC. Integration of this vector into the *M. smegmatis attB* site yielded strain dreemX, which yielded a positive SCC*mec* probe signal on the GeneXpert SANC. Black lines (single or double), chromosomal sequence; gray lines, sequence of the SCC*mec* insertion element; blue lines, vector elements; solid green boxes, *attB* and *attP* bacterial and phage attachment sites, respectively; open green boxes, *attL* and *attR* after insertion; green diamonds, pUC57-Simple multiple-cloning sites from GenScript; red color, location of GeneXpert SANC probes.

junction at the C terminus of *orfX* to confirm the presence of the mobile genetic cassette (Fig. 3A). We targeted this $attL_{SCC}$ junction for biomimicry. The MRSA-specific 960-bp sequence covering the $attL_{SCC}$ scar with *orfX* from *Staphylococcus aureus* subsp. *aureus* MW2 (480 bp, annotated in GenBank as MW_RS00130) followed by the first 480 bp of SCC*mec* (Fig. 3B) was chosen for delivery into the *M. smegmatis* chromosome using the same delivery method as for the $RRDR_{TB}$ (Fig. 3B). As the presence of the *mecA* gene is variable in clinical isolates (14), we excluded it from our strategy. The *spa* locus was also excluded, as we aimed to produce a first proof-of-principle biomimetic strain that targets the MRSA-dependent mobile element specifically. This approach resulted

TABLE 3 Results from the GeneXpert SA Nasal Complete assay[a]

Strain	Result	*spa*			SCC*mec*			*mecA*		
		C_T	Endpoint	Result	C_T	Endpoint	Result	C_T	Endpoint	Result
mc²155	MRSA negative; *S. aureus* negative	0	0	N[a]	0	3	N	0	7	N
dreemX	MRSA negative; *S. aureus* negative[b] (culture format)	0	1	N	25	460	P	0	4	N
	MRSA negative; *S. aureus* negative[b] (swab format)	0	1	N	21	459	P	0	-2	N

[a]All *M. smegmatis*-based strains are *spa* negative. N, negative (shaded); P, positive (not shaded).

[b]A negative result was obtained even though probe hybridization was positive for SCC*mec*. The embedded algorithms do not assign an SCC*mec* result as resistance because the disease-causing *S. aureus* is absent (no *spa* locus). For the purpose of this analysis, the SCC*mec* C_T and endpoint values are of interest, as they inform directly upon the utility of targeting one probe in a heterologous system using biomimicry.

in the production of strain dreemX (Fig. 3B). As expected, *M. smegmatis* mc²155 yielded a negative result with all probes in the GeneXpert-SANC assay (Table 3). In contrast, dreemX yielded a positive result for the SCC*mec* probe and negative results for the two targets (*spa* and *mec*), which were excluded from the biomimicry strategy (Table 3). The standard approach for sample preparation for the GeneXpert-SANC assay requires a cheek swab. To best replicate this, two formats were tested on dreemX, the first being an aliquot of culture and the second a cotton swab from a low density of cells plated on agar. In both cases, the expected probe pickup/dropouts were observed (Table 3).

DISCUSSION

The low growth rate of *M. tuberculosis* and difficulty in obtaining positive results from paucibacillary specimens constitute notable barriers to the effectiveness of culture-based diagnostics in the management of TB. In this context, the use of molecular diagnostics promises a greater capacity to rapidly diagnose and engage patients with effective health care. However, the deployment of these next-generation diagnostic tools within the health systems of countries where TB is endemic requires that careful attention be given the appropriate instrument verification and quality assurance mechanisms (6). In the absence of these, the use of molecular diagnostics in a point-of-care setting is seriously limited. To address this problem, dried culture spot (DCS) cards were introduced as verification material in the South African National Priority Program for TB (8), and this approach is rapidly gaining popularity globally. An analogous approach was also useful for verification of other TB molecular diagnostics, such as versions 1 and 2 of the LPA (18). Similarly, the European TB Reference Laboratory Network (ERLTB-Net) addressed external quality assessment (EQA) concerns across different laboratories and reported that implementation of verification systems allowed for consistency and comparison between labs (19). These studies highlight the importance of having verification material and mechanisms available for multicenter studies and accurate national reporting of TB incidence. Moreover, these systems strengthen the ability to provide high-quality near-patient or point-of-care diagnosis.

To verify TB NAAT-based diagnostic procedures, production of inactivated *M. tuberculosis* for distribution to participating laboratories requires the culture of pathogenic mycobacteria under biosafety level 3 (BSL3) conditions, leading to cost, time, and biosafety concerns, especially where drug-resistant strains are involved. The *M. smegmatis* strains developed and tested in this study were able to mimic the gene content of foreign DNA of *M. tuberculosis* and *S. aureus* origin. They were able to produce diagnostically valuable signals from the GeneXpert MTB/RIF and LPA technologies as expected, based on the NAAT nature of both assays. Hence, there is substantive clinical applicability of this methodology for EQA with modules at different and frequently remote locations. This approach also has the potential to complement in-house control procedures and other instrument verification modalities (6, 8, 19–22).

The emergence of drug-resistant TB is an important factor when considering instrument verification programs. Management of TB is compromised by the treatment of patients infected with resistant strains which are nonresponsive to antibiotics in the

regimen. In addition, these patients contribute to spread of resistant bacteria in communities. A large proportion of RIF-resistant strains are believed to be additionally resistant to INH (23, 24). In order for clinicians to make informed decisions, smear microscopy is not sufficient and ideally drug susceptibility testing (DST) needs to be performed alongside identification of the causative agent, *M. tuberculosis* (25, 26). In this context, NAATs are critical, and the biomimetic strains reported herein serve as ideal references to facilitate verification programs for drug-resistant TB.

The GeneXpert SA Nasal Complete assay was tested on the *M. smegmatis*-derived strain dreemX and was able to produce specific signal generated from probe SCC*mec*, which is present in MRSA strains containing SCC*mec*-integrating modules (15). Not all of these necessarily carry a *mecA* gene, so the SCC*mec* probe was chosen for this study. The results indicate that the protocol and associated cartridge from the GeneXpert SA Nasal Complete module is able to successfully lyse mycobacteria using the sonic lysis procedure. This suggests that the bacterial lysis procedure for the GeneXpert SA Nasal Complete module is sufficient to lyse mycobacteria also. The high G+C content (ca. 67% [27]) of mycobacterial DNA was of concern because of possible interference with the cycling and binding parameters optimized for *S. aureus*, which has a G+C content of ca. 33% (27). However, the difference between the G+C contents of *S. aureus* and *M. smegmatis* did not affect the results, suggesting that the annealing temperatures applied are highly specific for both the amplification steps and the probe hybridization, and the presence of mycobacterial DNA did not interfere with this. The high degree of specificity for the single SCC*mec* target included in the biomimetic *M. smegmatis* confirms that our approach is useful to construct highly selective verification standards that are target specific.

The work presented here demonstrates that *M. smegmatis*-derived strains can be used as surrogates for diagnostic assays that make use of NAAT technology, such as GeneXpert MTB/RIF and Hain LPA. These strains are potentially useful as standards for large-scale studies to eliminate variability due to site-specific in-house methods (19, 28, 29). The advantages of these strains are that they could be used to produce control EQA samples in a BSL2 facility. This (i) ensures that all samples have low biohazard content, (ii) requires staff trained only at BSL2, (iii) reduces the turnaround time required to produce batches of control samples, (iv) reduces the cost of production compared to those of BSL3 laboratories, and (v) allows for relatively simple gene editing to effectively mimic drug resistance. As demonstrated with the GeneXpert SA Nasal Complete assay, the application of this approach can be extended to other NAAT-based diagnostic purposes. Many new TB diagnostics are currently under development and being assessed by the WHO for applicability. The biomimetic reagents developed in this study are poised to make global impact in these diagnostic modalities.

MATERIALS AND METHODS

Bacterial strains and culture conditions. All strains and plasmids used and generated in this study are listed in Table 2. Cloning steps were performed in *Escherichia coli* strain DH5α, and the resulting shuttle plasmids were electroporated into *M. smegmatis* mc^{2}155 as previously described (30). *E. coli* strains were grown at 37°C in standard lysogeny broth (LB) or 2×YT rich culture liquid medium or on Luria agar (LA) supplemented with the appropriate antibiotics at concentrations of 100 to 200 μg/ml of ampicillin (Amp) or 200 μg/ml of hygromycin B (Hyg). *M. smegmatis* strains were grown at 37°C shaking in Middlebrook 7H9 liquid medium (Difco) supplemented with 0.085% NaCl, 0.2% glucose, 0.2% glycerol, and 0.05% Tween 80 or on Middlebrook 7H10 solid medium (Difco) supplemented with 0.085% NaCl, 0.2% glucose, and 0.5% glycerol. Hyg was used at 50 μg/ml.

Cloning of shuttle plasmids for integration into *M. smegmatis*. Plasmids were purchased from GenScript, with the 81-bp $RRDR_{TB}$ carried within a native fragment of 562 bp. For the *S. aureus* test, 960 bp of sequence specific to MRSA strains was included. Plasmids were digested with ScaI and NruI, releasing a fragment bearing the origin of replication with a disrupted *bla* gene and the sequence to be delivered. This was combined with a ScaI/NruI fragment from plasmid pHINT, bearing a cassette with the *hyg* gene for selection and the integrating L5-*int* mycobacteriophage element. Recombinant shuttle vectors were Amp^s and Hyg^r and capable of integration into the *M. smegmatis* chromosome at the *attB* locus.

Analysis of strains by standard GeneXpert laboratory diagnostics. Single colonies of wild-type or genetically modified *M. smegmatis* strains were picked and grown in liquid 7H9 medium supplemented with Hyg where appropriate. Bacteria were grown to stationary phase, and 300-μl volumes of 10-fold

dilutions from 10^2 to 10^5 were added to 3 ml of the SR lysis buffer supplied by the manufacturer. Samples were independently processed at the Clinical Laboratory Services facility based at the National Health Laboratory Service, Johannesburg, South Africa, in accordance with the manufacturer's instructions. GeneXpert MTB/RIF was used to test *M. tuberculosis* biomimetics and variants. The test for the SCC*mec* probe of MRSA using the GeneXpert SA Nasal Complete (GeneXpert-SANC) system was conducted at the National Health Laboratory Service, Charlotte Maxeke Academic Hospital, Johannesburg, South Africa. The biomimetic strain was added to 1 ml of the supplied buffer, either as 20 μl of stationary-phase liquid culture or as a single colony picked from solid medium. The cartridge was then processed in accordance with the manufacturer's instructions.

Analysis of strains by standard Hain Lifescience MTBDR*plus* LPA. Single colonies of mutant strains were picked from solid plates and suspended in 500 μl of molecular-biology-grade water. Samples were processed at the Clinical Laboratory Services facility at the National Health Laboratory Service, Johannesburg, South Africa. Results were scored visually from the hybridization strips and recorded as presence or absence of probe signal according to the manufacturer's instructions.

ACKNOWLEDGMENTS

This work was supported by funding from an International Early Career Scientist Award from the Howard Hughes Medical Institute (to B.D.K.), the South African National Research Foundation (to B.D.K.), the South African Medical Research Council (to B.D.K.), and a seed grant from Wits Enterprise (through the Technology Innovation Agency—South African Department of Science and Technology) at the University of the Witwatersrand (to B.D.K. and E.E.M.).

B.D.K. and E.E.M. conceived of the study, and E.E.M. executed the experimental work.

We thank Moagi Shaku for critical assessment of the manuscript.

We are involved in supporting SmartSpot Quality for the provision of verification reagents globally.

REFERENCES

1. Pai M, Furin J. 2017. Tuberculosis innovations mean little if they cannot save lives. eLife 6:25956.
2. Sulis G, Centis R, Sotgiu G, D'Ambrosio L, Pontali E, Spanevello A, Matteelli A, Zumla A, Migliori GB. 2016. Recent developments in the diagnosis and management of tuberculosis. NPJ Prim Care Respir Med 26:16078. https://doi.org/10.1038/npjpcrm.2016.78.
3. Bergmann JS, Woods GL. 1997. Mycobacterial growth indicator tube for susceptibility testing of *Mycobacterium tuberculosis* to isoniazid and rifampin. Diagn Microbiol Infect Dis 28:153–156. https://doi.org/10.1016/S0732-8893(97)00006-0.
4. Pai M, Minion J, Sohn H, Zwerling A, Perkins MD. 2009. Novel and improved technologies for tuberculosis diagnosis: progress and challenges. Clin Chest Med 30:701–716, viii. https://doi.org/10.1016/j.ccm.2009.08.016.
5. Migliori GB, Matteelli A, Cirillo D, Pai M. 2008. Diagnosis of multidrug-resistant tuberculosis and extensively drug-resistant tuberculosis: current standards and challenges. Can J Infect Dis Med Microbiol 19:169–172.
6. Stevens WS, Scott L, Noble L, Gous N, Dheda K. 2017. Impact of the GeneXpert MTB/RIF technology on tuberculosis control. Microbiol Spectr 5(1):TBTB2-0040-2016.
7. Heemskerk D, Caws M, Marais B, Farrar J. 2015. Springer briefs in public health: tuberculosis in adults and children, p 27–37. Springer, London, United Kingdom.
8. Scott LE, Gous N, Cunningham BE, Kana BD, Perovic O, Erasmus L, Coetzee GJ, Koornhof H, Stevens W. 2011. Dried culture spots for Xpert MTB/RIF external quality assessment: results of a phase 1 pilot study in South Africa. J Clin Microbiol 49:4356–4360. https://doi.org/10.1128/JCM.05167-11.
9. Stover CK, de la Cruz VF, Fuerst TR, Burlein JE, Benson LA, Bennett LT, Bansal GP, Young JF, Lee MH, Hatfull GF, Snapper SB, Barletta RG, Jacobs WR, Bloom BR. 1991. New use of BCG for recombinant vaccines. Nature 351:456–460. https://doi.org/10.1038/351456a0.
10. Rahman A, Sahrin M, Afrin S, Earley K, Ahmed S, Rahman SM, Banu S. 2016. Comparison of Xpert MTB/RIF assay and GenoType MTBDRplus DNA probes for detection of mutations associated with rifampicin resistance in *Mycobacterium tuberculosis*. PLoS One 11:e0152694. https://doi.org/10.1371/journal.pone.0152694.
11. Telenti A, Imboden P, Marchesi F, Lowrie D, Cole S, Colston MJ, Matter L, Schopfer K, Bodmer T. 1993. Detection of rifampicin-resistance mutations in *Mycobacterium tuberculosis*. Lancet 341:647–650. https://doi.org/10.1016/0140-6736(93)90417-F.
12. Koch A, Mizrahi V, Warner DF. 2014. The impact of drug resistance on *Mycobacterium tuberculosis* physiology: what can we learn from rifampicin? Emerg Microbes Infect 3:e17. https://doi.org/10.1038/emi.2014.17.
13. Aragón LM, Navarro F, Heiser V, Garrigo M, Espanol M, Coll P. 2006. Rapid detection of specific gene mutations associated with isoniazid or rifampicin resistance in *Mycobacterium tuberculosis* clinical isolates using non-fluorescent low-density DNA microarrays. J Antimicrob Chemother 57:825–831. https://doi.org/10.1093/jac/dkl058.
14. Turlej A, Hryniewicz W, Empel J. 2011. Staphylococcal cassette chromosome mec (Sccmec) classification and typing methods: an overview. Pol J Microbiol 60:95–103.
15. Holden MT, Feil EJ, Lindsay JA, Peacock SJ, Day NP, Enright MC, Foster TJ, Moore CE, Hurst L, Atkin R, Barron A, Bason N, Bentley SD, Chillingworth C, Chillingworth T, Churcher C, Clark L, Corton C, Cronin A, Doggett J, Dowd L, Feltwell T, Hance Z, Harris B, Hauser H, Holroyd S, Jagels K, James KD, Lennard N, Line A, Mayes R, Moule S, Mungall K, Ormond D, Quail MA, Rabbinowitsch E, Rutherford K, Sanders M, Sharp S, Simmonds M, Stevens K, Whitehead S, Barrell BG, Spratt BG, Parkhill J. 2004. Complete genomes of two clinical *Staphylococcus aureus* strains: evidence for the rapid evolution of virulence and drug resistance. Proc Natl Acad Sci U S A 101:9786–9791. https://doi.org/10.1073/pnas.0402521101.
16. Boundy S, Safo MK, Wang L, Musayev FN, O'Farrell HC, Rife JP, Archer GL. 2013. Characterization of the *Staphylococcus aureus* rRNA methyltransferase encoded by *orfX*, the gene containing the staphylococcal chromosome cassette mec (SCCmec) insertion site. J Biol Chem 288:132–140. https://doi.org/10.1074/jbc.M112.385138.
17. Katayama Y, Ito T, Hiramatsu K. 2000. A new class of genetic element, staphylococcus cassette chromosome *mec*, encodes methicillin resistance in *Staphylococcus aureus*. Antimicrob Agents Chemother 44:1549–1555. https://doi.org/10.1128/AAC.44.6.1549-1555.2000.
18. Gous N, Isherwood LE, David A, Stevens W, Scott LE. 2015. A pilot evaluation of external quality assessment of GenoType MTBDR*plus* versions 1 and 2 using dried culture spot material. J Clin Microbiol 53:1365–1367. https://doi.org/10.1128/JCM.03340-14.
19. Nikolayevskyy V, Hillemann D, Richter E, Ahmed N, van der Werf MJ, Kodmon C, Drobniewski F, Ruesch-Gerdes S, ERLTB-Net Network. 2016. External quality assessment for tuberculosis diagnosis and drug re-

sistance in the European Union: a five year multicentre implementation study. PLoS One 11:e0152926. https://doi.org/10.1371/journal.pone.0152926.
20. Boehme CC, Nabeta P, Hillemann D, Nicol MP, Shenai S, Krapp F, Allen J, Tahirli R, Blakemore R, Rustomjee R, Milovic A, Jones M, O'Brien SM, Persing DH, Ruesch-Gerdes S, Gotuzzo E, Rodrigues C, Alland D, Perkins MD. 2010. Rapid molecular detection of tuberculosis and rifampin resistance. N Engl J Med 363:1005–1015. https://doi.org/10.1056/NEJMoa0907847.
21. Blakemore R, Nabeta P, Davidow AL, Vadwai V, Tahirli R, Munsamy V, Nicol M, Jones M, Persing DH, Hillemann D, Ruesch-Gerdes S, Leisegang F, Zamudio C, Rodrigues C, Boehme CC, Perkins MD, Alland D. 2011. A multisite assessment of the quantitative capabilities of the Xpert MTB/RIF assay. Am J Respir Crit Care Med 184:1076–1084. https://doi.org/10.1164/rccm.201103-0536OC.
22. Gous N, Cunningham B, Kana B, Stevens W, Scott LE. 2013. Performance monitoring of *Mycobacterium tuberculosis* dried culture spots for use with the GeneXpert system within a national program in South Africa. J Clin Microbiol 51:4018–4021. https://doi.org/10.1128/JCM.01715-13.
23. Siddiqi SH, Aziz A, Reggiardo Z, Middlebrook G. 1981. Resistance to rifampicin and isoniazid in strains of *Mycobacterium tuberculosis*. J Clin Pathol 34:927–929. https://doi.org/10.1136/jcp.34.8.927.
24. World Health Organization. Treatment guidelines for drug-resistant tuberculosis, 2016 update. World Health Organization, Geneva, Switzerland.
25. Girosi F, Olmsted SS, Keeler E, Hay Burgess DC, Lim YW, Aledort JE, Rafael ME, Ricci KA, Boer R, Hilborne L, Derose KP, Shea MV, Beighley CM, Dahl CA, Wasserman J. 2006. Developing and interpreting models to improve diagnostics in developing countries. Nature 444(Suppl 1):S3–S8. https://doi.org/10.1038/nature05441.
26. McNerney R. 2015. Diagnostics for developing countries. Diagnostics (Basel) 5:200–209. https://doi.org/10.3390/diagnostics5020200.
27. Muto A, Osawa S. 1987. The guanine and cytosine content of genomic DNA and bacterial evolution. Proc Natl Acad Sci U S A 84:166–169. https://doi.org/10.1073/pnas.84.1.166.
28. Wolk DM, Struelens MJ, Pancholi P, Davis T, Della-Latta P, Fuller D, Picton E, Dickenson R, Denis O, Johnson D, Chapin K. 2009. Rapid detection of *Staphylococcus aureus* and methicillin-resistant S. aureus (MRSA) in wound specimens and blood cultures: multicenter preclinical evaluation of the Cepheid Xpert MRSA/SA skin and soft tissue and blood culture assays. J Clin Microbiol 47:823–826. https://doi.org/10.1128/JCM.01884-08.
29. Wolk DM, Picton E, Johnson D, Davis T, Pancholi P, Ginocchio CC, Finegold S, Welch DF, de Boer M, Fuller D, Solomon MC, Rogers B, Mehta MS, Peterson LR. 2009. Multicenter evaluation of the Cepheid Xpert methicillin-resistant *Staphylococcus aureus* (MRSA) test as a rapid screening method for detection of MRSA in nares. J Clin Microbiol 47:758–764. https://doi.org/10.1128/JCM.01714-08.
30. Gordhan BG, Parish T. 2001. Gene replacement using pretreated DNA. Methods Mol Med 54:77–92.
31. Ó Gaora P, Barnini S, Hayward C, Filley E, Rook G, Young D, Thole J. 1997. Mycobacteria as immunogens: development of expression vectors for use in multiple mycobacterial species. Med Princ Pract 6:91–96. https://doi.org/10.1159/000157432.
32. Snapper SB, Melton RE, Mustafa S, Kieser T, Jacobs WR, Jr. 1990. Isolation and characterization of efficient plasmid transformation mutants of *Mycobacterium smegmatis*. Mol Microbiol 4:1911–1919. https://doi.org/10.1111/j.1365-2958.1990.tb02040.x.